

# Non-standard adjoint problem in topology optimization using BEM in time harmonic elastodynamics

Peijun TANG<sup>1</sup>), Toshiro MATSUMOTO<sup>2</sup>), Kei MATSUSHIMA<sup>3</sup>), Hiroshi ISAKARI<sup>4</sup>), Toru TAKAHASHI<sup>5</sup>)

- 1) Nagoya University (Furo-cho, Chikusa-ku, Nagoya, Aichi, 464-8601, E-mail: tangpeijun@nuem.nagoya-u.ac.jp)  
 2) Nagoya University (Furo-cho, Chikusa-ku, Nagoya, Aichi, 464-8601, E-mail: t.matsumoto@nuem.nagoya-u.ac.jp)  
 3) Nagoya University (Furo-cho, Chikusa-ku, Nagoya, Aichi, 464-8601, E-mail: k\_matusima@nuem.nagoya-u.ac.jp)  
 4) Nagoya University (Furo-cho, Chikusa-ku, Nagoya, Aichi, 464-8601, E-mail: isakari@nuem.nagoya-u.ac.jp)  
 5) Nagoya University (Furo-cho, Chikusa-ku, Nagoya, Aichi, 464-8601, E-mail: ttaka@nuem.nagoya-u.ac.jp)

This paper presents a topology optimization problem with a strain-based objective functional on the boundary of the body for two-dimensional time-harmonic elastodynamics problems. An optimization method proposes a treatment of the integral term of the tangential derivatives of the displacement that cannot be treated directly in the conventional adjoint method. In the procedure of the optimization, configuration of the elastic materials is expressed by using the level set function, and the distribution of the level set function is iteratively updated according to the topological derivative. The topological derivative is associated with state and adjoint variables which are the solutions of the elastodynamics problem. In this paper, the elastodynamics problem are solved by a BEM solver. Along with the detailed formulas for topological derivative and BEM ( Boundary element method ), we present several numerical examples of inverse problem in elastodynamics, from which we've confirmed the validity of the presented method.

**Key Words:** Topology optimization, Level-set method, Topological derivatives, Boundary element method, Inverse problem, Strain-based objective function

## 1. Introduction

Suppressing and isolating the vibration of structures has long been an important issue in mechanical design, especially, in automobile, aviation, and shipbuilding industries.

With the development of computational mechanics and spread of CAE (computer aided engineering), designing mechanical products with high-performance now depends on computer simulations. Among all, as one of the most effective methods in generating the optimum structure, topology optimization has been proposed by Bendsøe and Kikuchi<sup>(1)</sup> in 1988 based on homogenization approach. Then, Bendsøe proposed a new approach<sup>(2)</sup> which is built on the basis of material distribution, the density method.

After that, various topology optimization schemes have been proposed based on homogenization and density method for elastic problems. Hagiwara et al.<sup>(3)</sup> proposed a method to maximize the eigenfrequency of isotropic and composite plates in three-dimensions using the homogenization method. Min et al.<sup>(4)</sup> proposed a method to minimize the dynamic elastic mean compliance in three-dimensions using the homogenization method. Yang et al.<sup>(5)</sup> proposed a method to minimize the elastic mean compliance in three-dimensions using the density method. Zhao et al.<sup>(6)</sup> investigated the effectiveness of the mode displacement method (MDM) and mode acceleration method (MAM) for time-domain response

problems within the framework of density-based topology optimization.

However, in dynamic problems and many other cases, a high stiffness design may result in low durability<sup>(5)</sup>, since the stress is not taken into consideration from the beginning, although the true optimum design of a structure largely depends on consideration of stresses.

In addition, for homogeneous method and density method, the intrinsic gray scale problem always results in blurred boundary which spoils the final results. To compensate the above defects, a level-set method has been proposed<sup>(7)(8)</sup> and introduced, which represents implicitly the target structural configurations by the iso-surface of the level set function. Shu et al.<sup>(9)</sup> proposed a method to minimize the displacement response at a specific point by using a shape optimization scheme based on the level-set method. Xia et al.<sup>(10)</sup> proposed a method to minimize the mean compliance of a structure with a material volume constraint by using level-set method for thermoelastic problems.

By switching to the level-set method and focusing on objective function composed by stresses or strains, genuine optimum design for mechanical parts can be achieved.

Stress-based optimization problems have long been a challenge in shape and topology optimization.<sup>(11)(12)(13)</sup> Stress optimization is one of the key factors for structural design in a wide range of engineering problems.<sup>(11)</sup>

---

Received Nov. 4, 2020, accepted Nov. 13, 2020

Li et al.<sup>(14)</sup> are the first who have applied isolation of stress through topology optimization with the help of level-set method. Luo et al.<sup>(15)</sup> conducted optimization upon stress-isolated hyperelastic composite structure. In a loaded structure, low stress levels are generally preferred, however, higher stress or strain can be really desired for specific small appliances like energy harvesters, and for design of failure prediction. And being directly related to stress, strain manipulation is also very practical in plenty of industrial applications.

In the present study, we develop a scheme for performing topology optimization for time-harmonic plane elastodynamics problems with the help of the level-set method for representing the shape of the material distribution. We consider an objective functional composed of tangential derivatives of the boundary displacements (strains). As the numerical analysis method, we use the boundary element method (BEM), which is very effective in solving wave propagation problems. As for the topology optimization, the method based on level set function proposed by Yamada et al.<sup>(16)</sup> is adopted. However, we develop a new approach to handle the objective functional based on boundary strain (tangential derivatives of displacements) by extending the conventional approach.

The paper is organized as follows. Section 2 presents the basic formulas of time-harmonic linear elastodynamics and related boundary element method used for solving the problem. Section 3 describes the process of obtaining the topological derivative and the derivation of strain-based adjoint problem. Section 4 demonstrates the verification of the derived topological derivative and presents several numerical examples of topology optimization. Section 5 gives the concluding remarks.

## 2. Boundary element method

### 2.1. Time-harmonic linear elastodynamic problem

Under the assumption of small deformation and linear elastic body, the relationships between the strain and the displacement, and the stress and the strain (Hooke's law) are given, respectively, as follows:

$$\varepsilon_{ij} = \frac{1}{2} (u_{i,j} + u_{j,i}), \quad (1)$$

$$\sigma_{ij} = C_{ijkl} \varepsilon_{kl}, \quad (2)$$

where  $u_i$  is the displacement vector,  $\varepsilon_{kl}$  is the strain tensor, and  $\sigma_{ij}$  is the stress tensor. For an isotropic elastic material,  $C_{ijkl}$  can be given as follows:

$$C_{ijkl} = \lambda \delta_{ij} \delta_{kl} + \mu (\delta_{ik} \delta_{jl} + \delta_{il} \delta_{jk}), \quad (3)$$

where  $\lambda$  and  $\mu$  are Lamé's constants and  $\delta_{ij}$  is Kronecker's delta.  $\lambda$  and  $\mu$  are related to Young's modulus  $E$  and Poisson's ratio  $\nu$  by

$$\lambda = \frac{\nu E}{(1-2\nu)(1+\nu)}, \quad (4)$$

$$\mu = \frac{E}{2(1+\nu)}. \quad (5)$$

Substituting Eqs.(1) and (3) into Eq.(2) yields Hooke's law relating the displacement gradients to the stress, as follows:

$$\sigma_{ij}(y) = \lambda \delta_{ij} u_{k,k} + 2\mu (u_{i,j} + u_{j,i}) \quad y \in \Omega. \quad (6)$$

The traction vector  $t_i$  on the boundary  $\Gamma$  can be expressed as follows,

$$t_i = \sigma_{ji} n_j = C_{ijkl} u_{k,l} n_j. \quad (7)$$

For time-harmonic linear elastodynamic problems, the governing differential equation and the boundary conditions are shown as follows:

$$C_{ijkl} u_{k,lj}(x) + \rho \omega^2 u_i(x) = 0, \quad x \in \Omega, \quad (8)$$

$$u_i(x) = \hat{u}_i(x), \quad x \in \Gamma_u, \quad (9)$$

$$t_i(x) = \hat{t}_i(x), \quad x \in \Gamma_t, \quad (10)$$

where summation convention is applied for repeated indices, and the indices after a comma denote differentiations with respect to the corresponding coordinates.  $\rho$  is the density of the material, and  $\omega$  is the circular frequency. Also,  $\Gamma = \Gamma_u \cup \Gamma_t$ .

### 2.2. Boundary element method

The displacement at a point  $y \in \Omega$  is related to the displacement and the traction on the boundary  $\Gamma$  by Somigliana's identity:

$$u_j(y) = \int_{\Gamma} U_{ij}(x, y) t_i(x) d\Gamma_x - \int_{\Gamma} T_{ij}(x, y) u_i(x) d\Gamma_x \quad y \in \Omega, \quad (11)$$

where  $U_{ij}$  are  $T_{ij}$  are the fundamental solution of Eq.(8) and the corresponding traction, respectively, and  $x$  is the point on boundary  $\Gamma$ .

For two-dimensional problems,  $U_{ij}$  and  $T_{ij}$  are given as follows<sup>(17)(18)</sup>:

$$U_{ij} = \frac{1}{2\pi\rho C_T^2} [\psi(r, s) \delta_{ij} - \kappa(r, s) r_i r_j], \quad (12)$$

$$T_{ij} = \frac{1}{2\pi} \left[ \left( \frac{d\psi(r, s)}{dr} - \frac{1}{r} \kappa(r, s) \right) \left( \delta_{ij} \frac{\partial r}{\partial n} - r_{,j} n_{,i} \right) + \frac{2}{r} \kappa(r, s) \left( r_{,i} n_{,j} + 2r_{,i} r_{,j} \frac{\partial r}{\partial n} \right) - 2 \frac{d\kappa(r, s)}{dr} r_{,i} r_{,j} \frac{\partial r}{\partial n} - \left( \frac{C_L^2}{C_T^2} - 2 \right) \left( \frac{d\psi(r, s)}{dr} - \frac{d\kappa(r, s)}{dr} - \frac{1}{r} \kappa(r, s) \right) r_{,i} n_{,j} \right], \quad (13)$$

where  $C_L$  and  $C_T$  are the speeds of the longitudinal and transverse waves, respectively,  $r$  is the distance between  $x$  and  $y$ ,  $n_i$  is the unit normal vector at  $x$ ,  $s = i\omega$  with the imaginary unit 'i', and

$$\psi(r, s) = K_0 \left( \frac{sr}{C_T} \right) + \frac{C_T}{sr} \left[ K_1 \left( \frac{sr}{C_T} \right) - \frac{C_T}{C_L} K_1 \left( \frac{sr}{C_L} \right) \right], \quad (14)$$

$$\kappa(r, s) = K_2 \left( \frac{sr}{C_T} \right) + \left( \frac{C_T}{C_L} \right)^2 K_2 \left( \frac{sr}{C_L} \right), \quad (15)$$

in which  $K_m$  ( $m = 0, 1, 2$ ) is the modified Bessel function of the second kind of  $m$ -th order.

By differentiating (11) with respect to  $y_i$ , the displacement gradient at  $y$  is obtained as

$$u_{j,i}(y) = \int_{\Gamma} \frac{\partial U_{ij}(x, y)}{\partial y_i} t_i(x) d\Gamma_x - \int_{\Gamma} \frac{\partial T_{ij}(x, y)}{\partial y_i} u_i(x) d\Gamma_x. \quad (16)$$

Thus, the stress components at  $y$  can be calculated by substituting (16) into Hooke's law (6).

The boundary integral equation is obtained by taking the limit of  $y \in \Omega$  tending to  $y \in \Gamma$ , as

$$c_{ij}u_i(y) + \int_{\Gamma} T_{ij}t(x,y)u_i(x)d\Gamma_x = \int_{\Gamma} U_{ij}(x,y)t_i(x)d\Gamma_x, \quad y \in \Gamma, \quad (17)$$

where  $c_{ij}$  is a constant determined by the shape of the boundary on which  $y$  is located. When  $y$  is at a smooth part of the boundary, we observe  $c_{ij} = \frac{1}{2}\delta_{ij}$ .

After discretization, Eq.(17) results in a system of linear algebraic equations, as follows:

$$[H] \{u\} = [G] \{t\}, \quad (18)$$

where  $\{u\}$  and  $\{t\}$  are the nodal vectors of the boundary displacement and traction, respectively, and  $[H]$  and  $[G]$  are the matrices obtained by evaluating the boundary integrals for each element.

By applying the boundary condition to Eq.(18) and transposing the unknown nodal values to the left-hand side, we obtain

$$[A] \{X\} = \{Y\}, \quad (19)$$

where,  $\{X\}$  is the vector consisting only of the unknown nodal values, and  $\{Y\}$  is the vector obtained by multiplying the vector consisting of the known nodal values to the corresponding coefficient matrix. After solving (19), all the nodal values of the displacement and the traction are obtained. Then, the displacement values at an arbitrary internal point in  $\Omega$  can be calculated by Eq.(11).

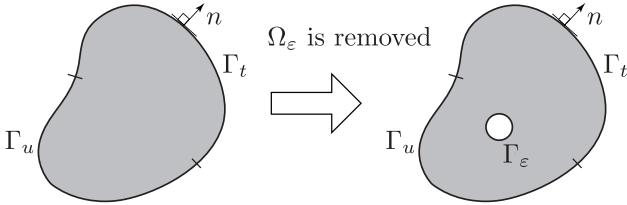


Fig. 1 Topology change when an infinitesimal cavity  $\Omega_\varepsilon$  appeared in elastic material region  $\Omega$ .

### 3. Topology optimization

#### 3.1. Derivation of topological derivative

As shown in Figure 1, it is assumed that the infinitesimal cavity is generated by removing an infinitesimal domain  $\Omega_\varepsilon$  from  $\Omega$ . Then, accordingly, the displacement  $u_i$  and the traction  $t_i$  change to  $u_i + \delta u_i$  and  $t_i + \delta t_i$ , respectively. After the appearance of the cavity corresponding to  $\Omega_\varepsilon$ , the displacement field  $u_i + \delta u_i$  is governed by the boundary value problem as follows,

$$C_{ijkl}(u_{k,lj}(x) + \delta u_{k,lj}(x)) + \rho\omega^2(u_i(x) + \delta u_i(x)) = 0, \quad x \in \Omega \setminus \Omega_\varepsilon \quad (20)$$

$$u_i(x) + \delta u_i(x) = \bar{u}_i(x), \quad x \in \Gamma_u, \quad (21)$$

$$t_i(x) + \delta t_i(x) = \bar{t}_i(x), \quad x \in \Gamma_t, \quad (22)$$

$$t_i(x) + \delta t_i(x) = 0, \quad x \in \Gamma_\varepsilon. \quad (23)$$

Apparently, we do not need to consider the case when an infinitesimal material appears in the domain out of the material because  $\delta u_i$  is not generated.

From the linearity of the problem, the following equations can be obtained through the subtractions of Eqs.(8) to (10) from Eqs.(20) to (23).

$$C_{ijkl}\delta u_{k,lj}(x) + \rho\omega^2\delta u_i(x) = 0, \quad x \in \Omega \setminus \Omega_\varepsilon, \quad (24)$$

$$\delta u_i(x) = 0, \quad x \in \Gamma_u, \quad (25)$$

$$\delta t_i(x) = 0, \quad x \in \Gamma_t, \quad (26)$$

$$\delta t_i(x) = -t_i(x), \quad x \in \Gamma_\varepsilon. \quad (27)$$

$\delta u_i$  is the variation of the displacement generated by removing an infinitesimal region  $\Omega_\varepsilon$  from the original domain  $\Omega$ .

In the conventional shape or topology optimization problems, the boundary type objective functional must have the following form

$$J = \int_{\Gamma} f(u_i, t_i) d\Gamma. \quad (28)$$

Equation (28) means that the objective functional consists only of the boundary displacement, which is the solution of the boundary value problem, and its corresponding traction which is another boundary quantity treated as the boundary condition. Because  $u_i$  and  $t_i$  are complex numbers and  $J$  takes real value, Eq.(28) actually have the following form:

$$J = \int_{\Gamma} f(u_i, u_i^*, t_i, t_i^*) d\Gamma, \quad (29)$$

where  $u_i^*$  and  $t_i^*$  are the complex conjugates of  $u_i$  and  $t_i$ , respectively. However, for simplicity, we write the objective functional in the form of Eq.(28) here.

After  $\Omega_\varepsilon$  is removed from  $\Omega$ , the objective functional suffers from a change  $\delta J$  as follows:

$$J + \delta J(\xi) = \int_{\Gamma} \left( f(u_i, t_i) + \frac{\partial f}{\partial u_i} \delta u_i + \frac{\partial f}{\partial t_i} \delta t_i \right) d\Gamma, \quad (30)$$

where  $\xi$  is the center of  $\Omega_\varepsilon$ . Recall that Eq.(30) in fact means

$$J + \delta J(\xi) = \int_{\Gamma} \left( f(u_i, u_i^*, t_i, t_i^*) + \frac{\partial f}{\partial u_i} \delta u_i + \frac{\partial f}{\partial u_i^*} \delta u_i^* + \frac{\partial f}{\partial t_i} \delta t_i + \frac{\partial f}{\partial t_i^*} \delta t_i^* \right) d\Gamma \quad (31)$$

By subtracting  $J$  of Eq.(28) from Eq.(30),  $\delta J(\xi)$  is obtained as follows:

$$\delta J(\xi) = \int_{\Gamma} \left( \frac{\partial f}{\partial u_i} \delta u_i + \frac{\partial f}{\partial t_i} \delta t_i \right) d\Gamma. \quad (32)$$

In order to evaluate  $\delta J(\xi)$ , by noticing  $\delta u_i$  is the solution of (24), it is necessary to evaluate  $\delta u_i$  on  $\Gamma$ . But it is not possible to do so for infinitely small  $\Omega_\varepsilon$ . In order to avoid evaluating  $\delta u_i$  on  $\Gamma$ , we try to eliminate the terms containing  $\delta u_i$  on  $\Gamma$  from  $J$ . Firstly, we start from the following Betti's reciprocal theorem between  $\delta u_i$  and  $\tilde{u}_i$  for  $\Omega \setminus \Omega_\varepsilon$  as follows:

$$\int_{\Gamma \cup \Gamma_\varepsilon} (\tilde{t}_i \delta u_i - \tilde{u}_i \delta t_i) d\Gamma = 0, \quad (33)$$

where  $\tilde{u}_i$  and  $\tilde{t}_i$  are the displacement and traction of another different load system for  $\Omega \setminus \Omega_\varepsilon$ .

By applying boundary conditions (25), (25), and (27) to Eq.(33), we can expand Eq.(33) as follows:

$$\begin{aligned} \int_{\Gamma \cup \Gamma_\varepsilon} (\tilde{t}_i \delta u_i - \tilde{u}_i \delta t_i) d\Gamma &= - \int_{\Gamma_u} \tilde{u}_i \delta t_i d\Gamma \\ &+ \int_{\Gamma_t} \tilde{t}_i \delta u_i d\Gamma + \int_{\Gamma_\varepsilon} (\tilde{t}_i \delta u_i + \tilde{u}_i t_i) d\Gamma = 0. \end{aligned} \quad (34)$$

For the purpose of removing  $\delta u_i$  and  $\delta t_i$  which cannot be evaluated on  $\Gamma$ , we consider the form obtained by subtracting Eq.(34) from Eq.(32) as

$$\begin{aligned} \delta J(\xi) &= \int_{\Gamma_u} \left( \tilde{u}_i + \frac{\partial f}{\partial t_i} \right) \delta t_i d\Gamma + \int_{\Gamma_t} \left( \frac{\partial f}{\partial u_i} - \tilde{t}_i \right) \delta u_i d\Gamma \\ &- \int_{\Gamma_\varepsilon} (\tilde{t}_i \delta u_i + \tilde{u}_i t_i) d\Gamma. \end{aligned} \quad (35)$$

In order to avoid the evaluation of  $\delta u_i$  on  $\Gamma_t$  and  $\delta t_i$  on  $\Gamma_u$ , we can use the solution of the following boundary value problem (adjoint problem) for  $\tilde{u}_i$  (adjoint displacement):

$$C_{ijkl} \tilde{u}_{k,lj}(x) + \rho \omega^2 \tilde{u}_i(x) = 0, \quad x \in \Omega, \quad (36)$$

$$\tilde{u}_i(x) = - \frac{\partial f(x)}{\partial t_i}, \quad x \in \Gamma_u \quad (37)$$

$$\tilde{t}_i(x) = \frac{\partial f(x)}{\partial u_i}, \quad x \in \Gamma_t. \quad (38)$$

Using the solution of the adjoint problem,  $\delta J(\xi)$  results in the integral only for  $\Gamma_\varepsilon$ , as follows:

$$\delta J(\xi) = - \int_{\Gamma_\varepsilon} \tilde{t}_i \delta u_i d\Gamma - \int_{\Gamma_\varepsilon} \tilde{u}_i t_i d\Gamma \quad (39)$$

Just like in the case of topology optimization of heat conduction problems,<sup>(19)</sup> by using the Taylor series expansions of  $u_i$  and  $\tilde{u}_i$  about the point at the center of  $\Omega_\varepsilon$ , and also using the asymptotic expansion of  $\delta u_i$  about the center of the cavity whose boundary is  $\Gamma_\varepsilon$ , we finally obtain the following expression of  $\delta J(\xi)$  (See Appendix).

$$\delta J(\xi) = (\pi \varepsilon^2) \mathcal{T}(\xi) + o(\varepsilon^2), \quad (40)$$

where  $\varepsilon$  is the radius of the infinitesimal circular cavity, and

$$\begin{aligned} \mathcal{T}(\xi) &= \text{Re} \left[ \frac{\lambda + 2\mu}{4\mu(\lambda + \mu)} (4\sigma_{ij}(\xi) \tilde{\sigma}_{ij}(\xi) - \sigma_{ii}(\xi) \tilde{\sigma}_{jj}(\xi)) \right. \\ &\left. - \rho \omega^2 u_i(\xi) \tilde{u}_i(\xi) \right]. \end{aligned} \quad (41)$$

Although the topological derivative for three-dimensional time-harmonic elastodynamic problems has been shown by Guizina et al.,<sup>(21)</sup> its two-dimensional expression is derived following their instruction (see Appendix).

### 3.2. Derivation of new adjoint problem for strain based topology optimization

For topology optimization considering stress on the boundary, we consider a simple objective functional  $J$  as follows:

$$J = \int_{\Gamma} f(\sigma_{ij}) d\Gamma. \quad (42)$$

Note that now the objective functional  $J$  does not contain  $u_i$  and  $t_i$  included in the standard boundary functional Eq.(28). By combining Eqs.(6) and (7), we find that the stress components on the boundary can be evaluated in terms of the

traction and the tangential derivative of the displacement as follows:

$$\sigma_{ij} = \alpha_{ijk} t_k + \beta_{ijk} u_{k,s}, \quad (43)$$

where

$$\alpha_{ijk} = \frac{1}{\lambda + 2\mu} [\lambda \delta_{ij} - 2(\lambda + \mu) n_i n_j] n_k + (\delta_{ik} n_j + \delta_{jk} n_i), \quad (44)$$

and

$$\begin{aligned} \beta_{ijk} &= \frac{2\lambda\mu}{\lambda + 2\mu} (\delta_{ij} - n_i n_j) s_k + \mu (\delta_{ik} - n_i n_k) s_j \\ &+ \mu (\delta_{jk} - n_j n_k) s_i. \end{aligned} \quad (45)$$

Thus, Eq.(42) can be considered as the objective functional consisting of the tangential derivative of the displacement instead and the traction as

$$J = \int_{\Gamma} (u_{i,s}, t_i) d\Gamma. \quad (46)$$

From the consideration similar to that of Eq.(32),  $\delta J(\xi)$  is written as follows:

$$\delta J = \int_{\Gamma} \left( \frac{\partial f}{\partial u_{i,s}} \delta u_{i,s} + \frac{\partial f}{\partial t_i} \delta t_i \right) d\Gamma. \quad (47)$$

Again, by subtracting Eq.(34) from (47), we obtain

$$\begin{aligned} \delta J &= \int_{\Gamma_u} \left( \frac{\partial f}{\partial t_i} + \tilde{u}_i \right) \delta t_i d\Gamma + \int_{\Gamma_t} \left( \frac{\partial f}{\partial u_{i,s}} \delta u_{i,s} - \tilde{t}_i \delta u_i \right) d\Gamma \\ &- \int_{\Gamma_\varepsilon} (\tilde{t}_i \delta u_i + \tilde{u}_i t_i) d\Gamma. \end{aligned} \quad (48)$$

The first term of the right-hand side of Eq.(48) contains  $\delta t_i$  as unknown variation of the traction on the boundary  $\Gamma_t$ , its evaluation can be avoided by considering the boundary condition for the adjoint displacement  $\tilde{u}_i$  as  $\tilde{u}_i = - \frac{\partial f}{\partial t_i}$  on  $\Gamma_t$ . However, the second term has  $\delta u_{i,s}$ , not  $\delta u_i$ , therefore, it is not possible to consider an appropriate boundary condition for  $\tilde{t}_i$  on  $\Gamma_t$ . Therefore, we integrate by parts the term having  $\delta u_{i,s}$  for the boundary  $\Gamma_t$  on which the traction is specified as the boundary condition, as follows:

$$\begin{aligned} \int_{\Gamma_t} \frac{\partial f}{\partial u_{i,s}} \delta u_{i,s} d\Gamma &= \int_{\Gamma_t} \frac{\partial f}{\partial u_{i,s}} \frac{\partial}{\partial s} (\delta u_i) d\Gamma \\ &= \left( \frac{\partial f}{\partial u_{i,s}} \delta u_i \right) \Big|_Q^P - \int_{\Gamma_t} \frac{\partial}{\partial s} \left( \frac{\partial f}{\partial u_{i,s}} \right) \delta u_i d\Gamma \end{aligned} \quad (49)$$

Here,  $P$  and  $Q$  denote the start and end points of the boundary  $\Gamma_t$  which is a part of the boundary. With this, the variation of  $J$  now can be written as

$$\begin{aligned} \delta J &= \int_{\Gamma_u} \left( \frac{\partial f}{\partial t_i} + \tilde{u}_i \right) \delta t_i d\Gamma - \int_{\Gamma_t} \left( \frac{\partial}{\partial s} \left( \frac{\partial f}{\partial u_{i,s}} \right) + \tilde{t}_i \right) \delta u_i d\Gamma \\ &- \int_{\Gamma_\varepsilon} (\tilde{t}_i \delta u_i + \tilde{u}_i t_i) d\Gamma + \left( \frac{\partial f}{\partial u_{i,s}} \delta u_i \right) \Big|_Q^P. \end{aligned} \quad (50)$$

Now we find that the second integral containing  $\delta u_i$  on the right-hand side of the above equation can be eliminated by considering an appropriate boundary condition for  $\tilde{t}_i$ . Instead, the last term containing  $\delta u_i$  at the extreme points of  $\Gamma_t$  now appears. In order to eliminate it, we can use an interpolation of  $\frac{\partial f}{\partial u_{i,s}}$  so that its value becomes zero at  $P$  and  $Q$ .

Because the essential difference between the present problem and the conventional problem is the existence of  $u_{i,s}$  in the boundary functional  $f$ , we consider, in the present study,  $J$  having the following form of  $f$ :

$$J = \int_{\Gamma} f(u_{i,s}, \bar{u}_{i,s}) d\Gamma, \quad (51)$$

where  $u_{i,s} = \frac{\partial u_i}{\partial s}$ , and  $\bar{u}_{i,s}$  is the target tangential derivative which should be achieved after the topology optimization.

Let us assume that  $u_i$  is interpolated using shape functions such as quadratic ones. Under the above treatment, the last term of the right-hand side of Eq.(50) can be neglected. Its first and second terms can be eliminated by considering the following adjoint problem:

$$C_{ijkl}\tilde{u}_{k,lj}(x) + \rho\omega^2\tilde{u}_i(x) = 0, \quad x \in \Omega, \quad (52)$$

$$\tilde{u}_i(x) = -\frac{\partial f}{\partial t_i}(x), \quad x \in \Gamma_u \quad (53)$$

$$\tilde{t}_i(x) = -\frac{\partial}{\partial s} \left( \frac{\partial f}{\partial u_{i,s}}(x) \right), \quad x \in \Gamma_{t^o}, \quad (54)$$

where  $\Gamma_{t^o}$  denotes the extended  $\Gamma_t$  whose extreme points have no value of  $\frac{\partial f}{\partial u_{i,s}}$ .

### 3.3. Topology optimization using shape representation by level-set method

Level-set method is an approach that uses a scalar function (level set function  $\phi(x)$ ) to represent the shape of the material. As shown in Figure 2,  $\phi(x)$  is defined by

$$\begin{cases} 0 < \phi(x) \leq 1 & (x \in \Omega) \\ \phi(x) = 0 & (x \in \Gamma) \\ -1 \leq \phi(x) < 0 & (x \in D \setminus \Omega) \end{cases} \quad (55)$$

where  $D$  denotes the fixed design domain and  $\Omega$  the material part outside the cavity. By introducing the level set function  $\phi(x)$ , the problem of topology optimization is now changed to that of searching the optimum distribution of  $\phi(x)$  that minimizes the objective functional.

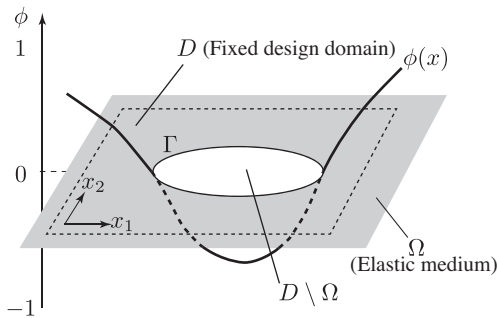


Fig. 2 Shape expression by level set function.

The present topology optimization problem is given by an augmented objective functional as shown below,

$$\inf_{\phi} J = \int_{\Gamma} f(u_{i,s}) d\Gamma + \int_{\Omega} \tilde{u}_i(C_{ijkl}u_{k,lj} + \rho\omega^2 u_i) d\Omega + \lambda G, \quad (56)$$

where

$$G = \int_{\Omega} d\Omega - V_{\max} \leq 0. \quad (57)$$

The evolution of the level set function in accordance with the change in the shape and topology of the material distribution is assumed to follow an evolution equation:<sup>(16)</sup>

$$\frac{\partial \phi(x,t)}{\partial t} = K (\mathcal{T}(x,t) - \lambda + \tau \nabla^2 \phi(x,t)) \quad (x \in D), \quad (58)$$

$$\phi(x,0) = \phi_0 \quad (x \in D), \quad (59)$$

$$\phi(x,t) = c \quad (x \in \partial D), \quad (60)$$

where  $K$  is an appropriate positive constants, and  $t$  denotes the introduced fictitious time, which may not be confused with the traction.  $\tau$  is a regularization parameter of positive constant to control the mean curvature distribution of  $\phi(x)$ . For a large value of  $\tau$ , the obtained topological shape of the material distribution is going to be more simpler.<sup>(16)</sup>

Equation (58) is calculated for updating the distribution of  $\phi(x)$  iteratively to find the optimum topology.

### 3.4. Computational procedure

Equation (58) can be solved by using the finite element method easily because the fixed design domain  $D$  is kept to be the same for all the shape modification processes. Thus, the finite element mesh and the corresponding stiffness matrix are always the same. However, from the iso-surface for  $\phi(x) = 0$ , the boundary shape of the material is extracted<sup>(20)</sup> and the boundary elements are generated to use for the time-harmonic elastodynamic BEM analysis for the primary and adjoint problems. The entire computation algorithm of the present topology optimization is shown in Figure 3.

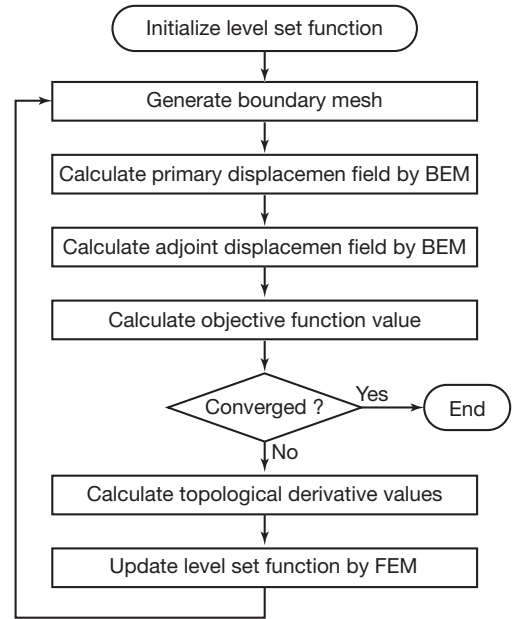


Fig. 3 Computation flow of present topology optimization procedure.

## 4. Numerical examples

### 4.1. Verification of topological derivative

The topological derivative derived in this study is first verified through the comparison with those computed by a finite difference approximation of the topological derivative. For this purpose, an objective functional is defined.

Consider a square plate under uniform tensile tractions of  $1.0 \times 10^9$  as shown in Figure 4. Material constants are set

to be  $E = 2.16 \times 10^{10}$  [Pa],  $\nu = 0.3$ , and  $\rho = 7850$  [kg/m<sup>3</sup>] throughout all the numerical examples. The tangential derivative of the displacement  $\bar{u}_{i,s}$  on all the boundaries of the plate without a cavity can be easily obtained for this problem. The objective functional is defined as

$$J = \int_{\Gamma} (u_{i,s} - \bar{u}_{i,s})(u_{i,s}^* - \bar{u}_{i,s}^*) d\Gamma \quad (61)$$

We verify the topological derivative  $\mathcal{T}$  of the explicit form of Eq.(41) by comparing it with a finite difference approximation of the objective value between that calculated without an actual small circular hole and that without any hole, i.e.,

$$\mathcal{T} = \frac{J_{\text{hole}} - J_{\text{orig}}}{\pi \varepsilon^2} \quad (62)$$

where  $J_{\text{hole}}$  is the calculated value of the objective functional when a small hole is placed and  $J_{\text{orig}}$  is for the original state without any hole.  $\varepsilon$ , the radius of the actual small hole, is set to be 0.2 and its boundary is divided into 16 quadratic boundary elements. The topological derivative values at the points along the lines A, B, and C are compared with the approximate values by placing the small holes along these lines. Line A is along  $x_1$ -axis, line B is along  $x_2 = -0.3$ , and line C is along  $x_2$ -axis.

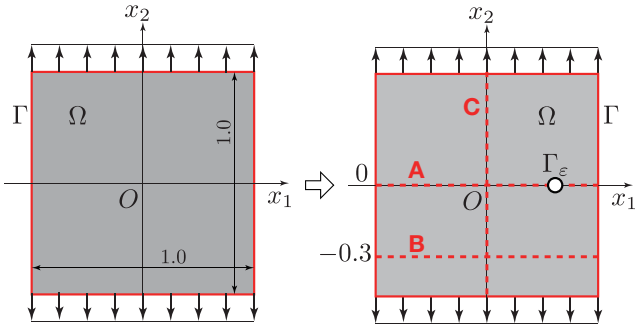


Fig. 4 Verification of topological derivative.

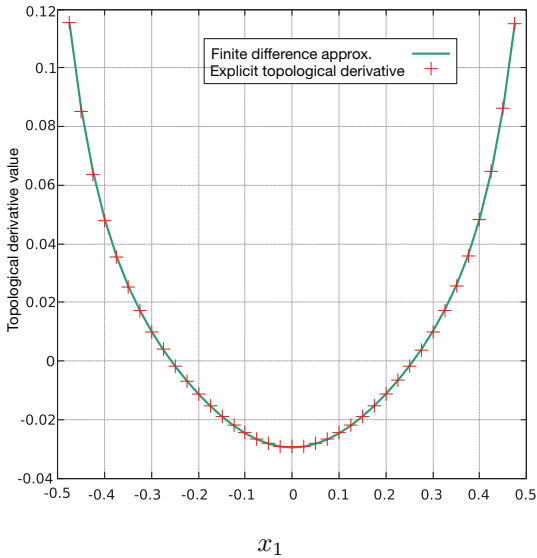


Fig. 5 Topological derivative values along line A.

In Figs.5 to 7, the topological derivative values calculated by its explicit expression of Eq.(41) are compared with those calculated by the finite difference approximation of the objective functional values of Eq.(62). The green line denotes

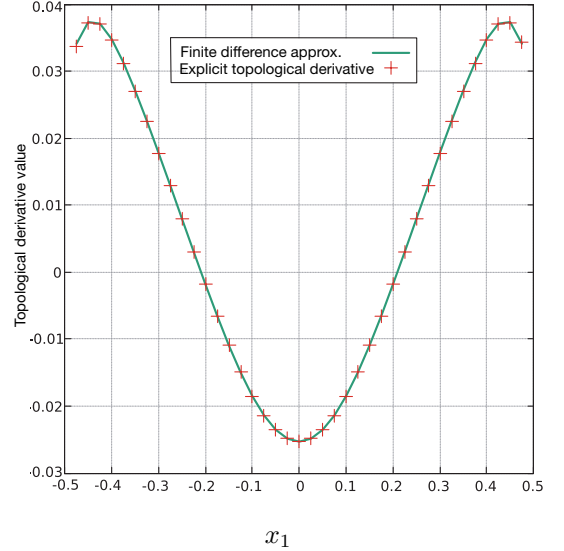


Fig. 6 Topological derivative values along line B.

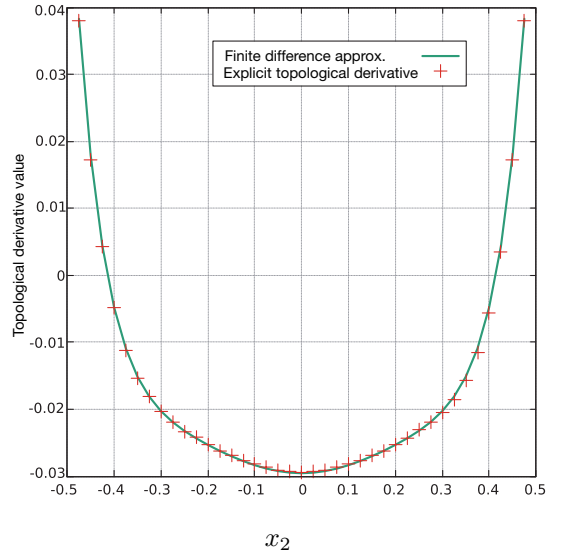


Fig. 7 Topological derivative values along line C.

the values of finite difference approximation, and the red cross dot denotes the adopted explicit expression of topological derivative  $\mathcal{T}$ . The results obtained by using Eq.(41) show good agreements with those obtained by the finite difference approximation results, demonstrating the validity of the derived topological derivative expression of Eq.(41).

#### 4.2. Example topology optimization problems with boundary functionals of displacement gradients

The validity of the proposed method is demonstrated through some numerical examples constructed by using the tangential derivatives of the displacement calculated for several different cavities in the square region as shown in Figure 8.

First, we consider a problem having a cavity in the domain and calculate the displacement gradients on the boundary of the square region. On the upper and lower edge boundaries, the tangential derivatives of the displacements correspond to  $u_{1,1}$ , and on the side edge boundaries, they correspond to  $u_{2,2}$ . By considering these displacement gra-



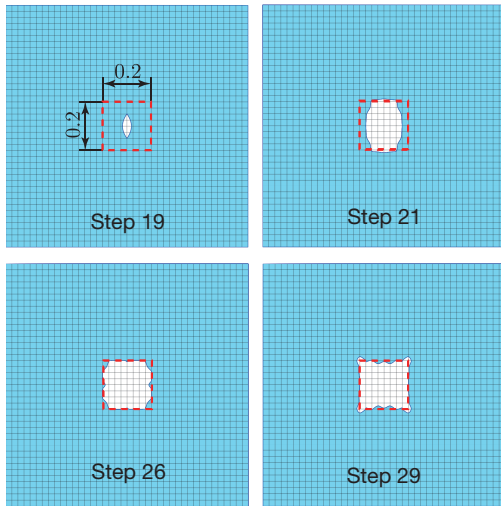


Fig. 11 Results of topology optimization for a square target cavity.

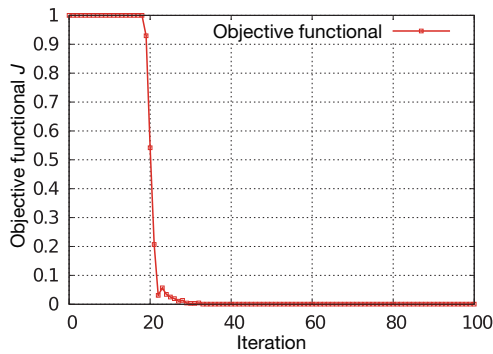


Fig. 12 History of the value of objective functional for topology optimization with a square target cavity.

#### 4.2.3. Topology optimization corresponding to detecting a triangular cavity

As the third numerical example, we consider a topology optimization problem whose optimum cavity shape is a triangle. The geometry setting for the targeting triangular cavity is given as follows:

- Three interior angles of the triangular cavity are  $50^\circ$ ,  $60^\circ$ , and  $70^\circ$ .
- The base of the triangle is rotated around its incenter by  $15^\circ$  in counterclockwise direction.
- The radius of the triangular cavity's inscribed circle is 0.12.
- The incenter of the triangular cavity is consistent with the center of the square design domain.

Figure 13 shows the iterative process of topology optimization. An oval cavity first appeared slightly away from the incenter of the target triangle. Then, at step 14, the appeared cavity grew larger and shifted to the incenter but its shape became rather complicated. Then, the cavity shape approached the triangular one and finally fit the target triangular shape well.

The history of the change of the objective functional value is shown in Figure 14. The initial value of the objective functional was  $J_{\text{initial}} = 0.151078 \times 10^{-2}$  and its final

value was  $J_{\text{final}} = 0.179182 \times 10^{-5}$ . Also in this example, about 99% reduction of  $J_{\text{initial}}$  was achieved.

Also in this example, the target triangular shape has three corners, but the obtained cavity having the round boundaries at the assumed vertices of the triangle looks close enough to a triangle.

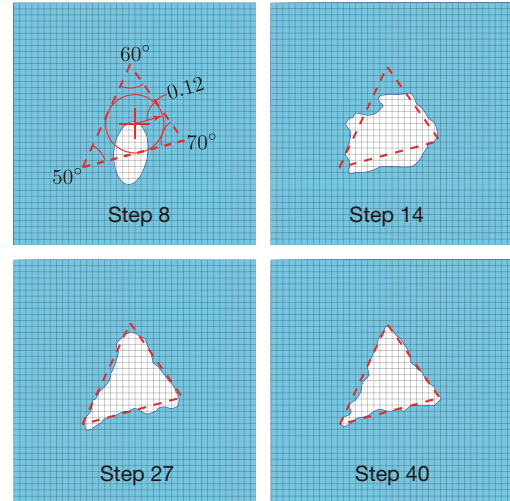


Fig. 13 Results of topology optimization for a triangular target cavity.

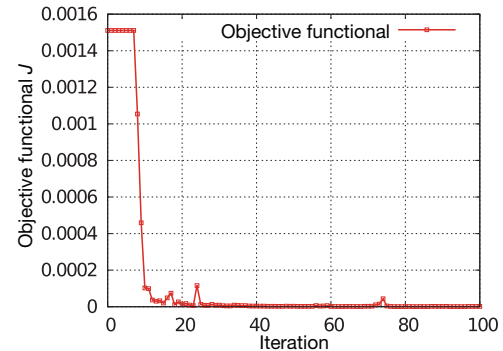


Fig. 14 History of the value of objective functional for topology optimization with a triangular target cavity.

#### 4.2.4. Topology optimization corresponding to detecting a oval cavity

As the final example, we consider the case of an oval cavity detection. And the geometry settings for the targeting oval cavity is given as follows:

- The center of the oval cavity is consistent with the center of the design domain.
- The length of the oval cavity's long axis is 0.22, while its short axis is 0.10.
- The oval cavity is rotated around its center by  $30^\circ$  in clockwise direction.

Again, in Figure 15 is shown the process of topology optimization for targeting oval-shape cavity. The appeared cavity was a slender ellipse but its long axis was oriented to  $x_2$  direction. At step 12, the cavity expanded more than the targeting cavity, but after step 23, the appeared cavities were almost the same as the oval cavity which was targeted.

As shown in Figure 16, the convergence was quick. The initial value of the objective functional was  $J_{\text{initial}} = 0.151078 \times 10^{-2}$ , while its final value was  $J_{\text{final}} = 0.179182 \times 10^{-5}$ . About 99% reduction of  $J_{\text{initial}}$  was observed.

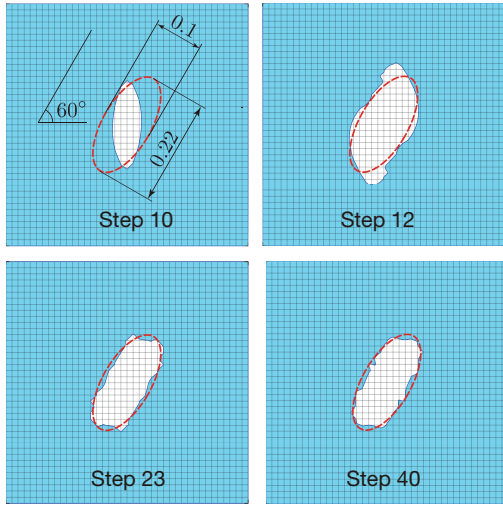


Fig. 15 Results of topology optimization for a oval target cavity.

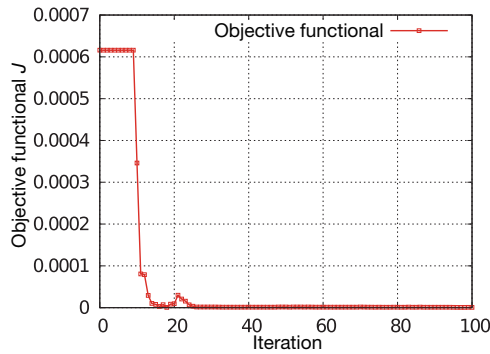


Fig. 16 History of the valued of objective functional for topology optimization with a oval target cavity.

## 5. Concluding remarks

In the present study, a treatment of the topology optimization whose boundary functional consists of tangential derivatives of displacements. The problem is associated with the boundary stress-base shape and topology optimization. To derive the adjoint problem which enables the elimination of the variation of tangential derivative of displacement vector, integration by parts of the tangential derivative was applied. By using the solution of this adjoint problem, the topological derivative can be derived and used for topology optimization problems. The derived topological derivative was verified by comparing with that calculated based on the finite difference approximation of the change of the objective functional. Some numerical examples of topology optimization problems whose optimum shapes are know were shown and the effectiveness of the present approach has been demonstrated. The drawback of the present formulation is that there exist the term related to the variations of the displacement gradients at the extreme points of the boundary on which the boundary functional of the displacement gradi-

ents is specified. The present approach avoided the evaluation of them by employing an interpolation with which those values vanish at the extreme points, but further studies are needed to improve this drawback.

## Acknowledgement

This work was partially supported by the Grant-in-Aid for Scientific Research (A), No.19H00740, of the Japan Society for the Promotion of Science.

## References

- (1) M.P. Bendsøe, N. Kikuchi, Generating optimal topologies in structural design using a homogenization method. *Computer Methods in Applied Mechanics and Engineering*, Vol. 71, pp. 197–224, 1988.
- (2) M.P. Bendsøe, Optimal shape design as a material distribution problem. *Structural optimization*, Vol. 1, pp. 193–202, 1989.
- (3) H.L. Tenek, I. Hagiwara, Eigenfrequency maximization of plates by optimization of topology using homogenization and mathematical programming. *JSME International Journal. Ser. C, Dynamics, Control, Robotics, Design and Manufacturing*, Vol. 37, Issu 4, pp.667–677, 1994.
- (4) S. Min, N. Kikuchi, Y.C. Park, S. Kim and S. Chang Optimal topology design of structures under dynamic loads. *Structural and Multidisciplinary Optimization*, 17(1999) , pp. 208–218.
- (5) R.J. Yang, C.J. Chen, Stress-based topology optimization. *Structural Optimization Journal*, Vol. 12, pp. 98–105, 1996.
- (6) Junpeng Zhao, Chunjie Wang, Dynamic response topology optimization in the time domain using model reduction method. *Structural and Multidisciplinary Optimization*, Vol.53, pp. 101–114, 2016.
- (7) M.Y. Wang, X. Wang, D. Guo, A level set method for structural topology optimization. *Computer methods in applied mechanics and engineering*, Vol. 192, pp.227–246, 2003.
- (8) G. Allaire, F. Jouve, A.M. Toader, Structural optimization using sensitivity analysis and a level-set method. *Journal of computational physics*, Vol. 194, pp. 363–393, 2004.
- (9) L. Shu, M.Y. Wang, Z. Fang, Z.-D. Ma, P. Wei, Level set based structural topology optimization for minimizing frequency response. *Sound and Vibration*, Vol. 330, pp. 5820–5834, 2011.
- (10) Q. Xia, M.Y. Wang, Topology optimization of thermoelastic structures using level set method. *Computational Mechanics*, Vol.42, Article number: 837, 2008,
- (11) R. Picelli, S.Townsend, C. Brampton, J. Norato, H.A. Kim, Stress-based shape and topology optimization with the level set method. *Computer Method in Applied Mechanics and Engineering*, Vol. 329, pp. 1–29, 2017.

- (12) P. Duysinx, M.P. Bense, Topology optimization of continuum structures with local stress constraints. *International journal for numerical methods in engineering*, Vol.43, pp.1453–1478, 1998.
- (13) P. Duysinx, L.V. Miegroet, E. Lemaire, O. Bruls, M. Bruyneel, Topology and generalized shape optimization: Why stress constraints are so important? *International Journal for Simulation and Multidisciplinary Design Optimization*, Vol. 2, pp. 253–258, 2008.
- (14) L. Li, M.Y. Wang, Stress isolation through topology optimization. *Structural and Multidisciplinary Optimization*, Vol. 49, pp. 761–769, 2014.
- (15) Y. Luo, M. Li, Z. Kang, Optimal topology design for stress-isolation of soft hyperelastic composite structures under imposed boundary displacements. *Structural and Multidisciplinary Optimization*, Vol. 55, pp. 1747–1758, 2017.
- (16) T. Yamada, K. Izui, S. Nishiwaki, A. Takezawa, A topology optimization method based on the level set method incorporating a fictitious interface energy. *Computer Methods in Applied Mechanics and Engineering*, Vol. 199, pp. 2876–2891, 2010.
- (17) T.A. Cruse and F.J.A. Rizzo, Direct Formulation and Numerical Solution of the General Transient Elastodynamic Problem I. *Journal of Mathematical Analysis and Applications*, Vol. 22, pp. 244–259, 1968.
- (18) T.A. Cruse, A direct formulation and numerical solution of the general transient elastodynamic problem II. *Journal of Mathematical Analysis and Applications*, Vol. 22, pp. 341–355, 1968.
- (19) G. Jing, H. Isakari, T. Matsumoto, T. Takahashi, Level set-based topology optimization for 2D heat conduction problems using BEM with objective function defined on design-dependent boundary with heat transfer boundary condition. *Engineering Analysis with Boundary Elements*, Vol. 61, pp. 61–70, 2015.
- (20) T. Matsumoto, T. Yamada, S. Shichi, T. Takahashi, A study on topology optimization using the level-set function and BEM. *Boundary Elements and Other Mesh Reduction Methods*, Vol. 34, pp. 123–133, 2012.
- (21) Guzina, B.B., Bonnet, M., Topological derivative for the inverse scattering of elastic waves, *The Quarterly Journal of Mechanics and Applied Mathematics*, Vol. 57(2), pp. 161–179, 2004, <https://doi.org/10.1093/qjmam/57.2.161>.

## Appendix

The variation of objective functional  $\delta J$  shown in Eq.(39) is shown again as

$$\delta J = - \int_{\Gamma_\varepsilon} \tilde{t}_i \delta u_i d\Gamma - \int_{\Gamma_\varepsilon} \tilde{u}_i t_i d\Gamma \quad (64)$$

In order to evaluate the integrals on the right-hand side of the above expression, we need the behaviors of  $t_i$ ,  $\tilde{u}_i$ ,  $\tilde{t}_i$  in the neighborhood of the center of  $\Omega_\varepsilon$  before  $\Omega_\varepsilon$  is removed from  $\Omega$ , as shown in Figure 17 and the asymptotic expansion

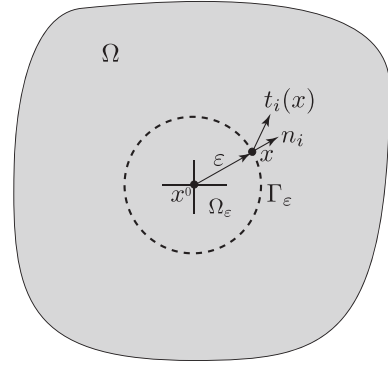


Fig. 17 The neighborhood of small circular region centered ad  $x^0$ .

of  $\delta u_i$  about the center of  $\Gamma_\varepsilon$ .

First, we evaluate the second integral of Eq.(64).

$$\begin{aligned} \int_{\Gamma_\varepsilon} \tilde{u}_i t_i d\Gamma &= \int_{\Gamma_\varepsilon} C_{ijkl} u_{k,l} \tilde{u}_i n_j d\Gamma \\ &= - \int_{\Omega_\varepsilon} (C_{ijkl} u_{k,lj} \tilde{u}_i + C_{ijkl} u_{k,l} \tilde{u}_{i,j}) d\Omega \\ &= \int_{\Omega_\varepsilon} (\rho \omega^2 u_i \tilde{u}_i - D_{ijkl} \sigma_{ij} \tilde{\sigma}_{kl}) d\Omega, \end{aligned} \quad (65)$$

where the outward unit normal vector is  $-n_i$  for  $\Omega_\varepsilon$ . The strain and the adjoint strain are related to the corresponding stresses as follows:

$$\varepsilon_{ij}(x) = D_{ijkl} \sigma_{kl}(x), \quad (66)$$

$$\tilde{\varepsilon}_{ij}(x) = D_{ijkl} \tilde{\sigma}_{kl}(x). \quad (67)$$

where  $D_{ijkl}$  is the compliance tensor and is given as

$$D_{ijkl} = - \frac{\lambda}{4\mu(\lambda + \mu)} \delta_{ij} \delta_{kl} + \frac{1}{4\mu} (\delta_{ik} \delta_{jl} + \delta_{il} \delta_{jk}) \quad (68)$$

$u_i(x)$ ,  $\tilde{u}_i(x)$ ,  $\sigma_{ij}(x)$ , and  $\tilde{\sigma}_{ij}(x)$  are the quantities for the domain before  $\Omega_\varepsilon$  is removed, we consider their Taylor series expansion about the center  $x^0$  of  $\Omega_\varepsilon$ , as shown in Figure 17 then we observe

$$u_i(x) = u_i^0 + O(\varepsilon), \quad (69)$$

$$\tilde{u}_i(x) = \tilde{u}_i^0 + O(\varepsilon), \quad (70)$$

$$\sigma_{ij}(x) = \sigma_{ij}^0 + O(\varepsilon), \quad (71)$$

$$\tilde{\sigma}_{ij}(x) = \tilde{\sigma}_{ij}^0 + O(\varepsilon), \quad (72)$$

where

$$u_i^0 = u_i(x^0), \quad \tilde{u}_i^0 = \tilde{u}_i(x^0), \quad (73)$$

$$\sigma_{ij}^0 = \sigma_{ij}(x^0), \quad \tilde{\sigma}_{ij}^0 = \tilde{\sigma}_{ij}(x^0). \quad (74)$$

Substituting Eqs.(69) to Eq.(72) into Eq.(65), finally we obtain

$$\begin{aligned} \int_{\Gamma_\varepsilon} \tilde{u}_i t_i d\Gamma &= \pi \varepsilon^2 (\rho \omega^2 u_i^0 \tilde{u}_i^0 - D_{ijkl} \sigma_{ij}^0 \tilde{\sigma}_{kl}^0) + O(\varepsilon^3) \\ &= \pi \varepsilon^2 \left( \rho \omega^2 u_i^0 \tilde{u}_i^0 + \frac{\lambda}{4\mu(\lambda + \mu)} \sigma_{ii}^0 \tilde{\sigma}_{jj}^0 - \frac{1}{2\mu} \sigma_{ij}^0 \tilde{\sigma}_{ij}^0 \right) + O(\varepsilon^3) \end{aligned} \quad (75)$$

Next, the first term of the right-hand side of Eq.(39) is evaluated.

The neighborhood of the circular cavity centered at  $x_0$  is shown in Figure 18. Note that the direction of the unit outward normal vector is opposite to that of the boundary of  $\Omega_\varepsilon$  shown in Figure 17 and that  $\tilde{t}_i$  is the traction at a point  $x$  on the boundary of  $\Omega_\varepsilon$  defined with that normal vector.

The variation of the displacement  $\delta u_i$  is the solution of the following boundary value problem.

$$C_{ijkl}\delta u_{k,lj}(x) + \rho\omega^2\delta u_i(x) = 0, \quad x \in \Omega \setminus \Omega_\varepsilon \quad (76)$$

$$\delta t_i(x) = -t_i(x), \quad x \in \Gamma_\varepsilon \quad (77)$$

$$\delta u_i(x) = 0, \quad x \in \Gamma_u, \quad (78)$$

$$\delta t_i(x) = 0, \quad x \in \Gamma_t. \quad (79)$$

In what follows, the behavior of  $\delta u_i(x)$  in the neighborhood of  $\Gamma_\varepsilon$  is investigated. Due to the boundary condition (77), we have

$$\delta t_i(x) = -t_i(x), \quad x \in \Gamma_\varepsilon. \quad (80)$$

Note again that  $t_i$  above is defined with the stress components for  $\Omega_\varepsilon$  and the normal vector on  $\Gamma_\varepsilon$ .

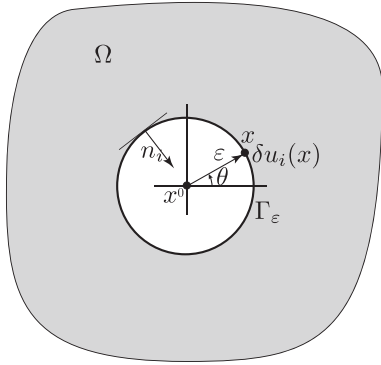


Fig. 18 The neighborhood of small circular cavity centered at  $x^0$ .

By taking the origin of the coordinate system to  $x^0$ , the coordinate components of the point  $x$  on  $\Gamma_\varepsilon$  can be written using the polar coordinate as follows:

$$x_1 = r \cos\theta \quad (81)$$

$$x_2 = r \sin\theta \quad (82)$$

Because  $\delta u_i(x)$  is the solution of the governing differential equation (76), its asymptotic expansion about  $x^0$  and corresponding traction can be obtained using the above polar coordinates, as follows:

$$\delta u_r(x) = \frac{1}{r} \sum_{n=-\infty}^{\infty} (a_n U_1^n(r) + b_n U_2^n(r)) e^{in\theta}, \quad (83)$$

$$\delta u_\theta(x) = \frac{1}{r} \sum_{n=-\infty}^{\infty} (a_n V_1^n(r) + b_n V_2^n(r)) e^{in\theta}, \quad (84)$$

$$\delta t_r(x) = -\frac{2\mu}{\varepsilon^2} \sum_{n=-\infty}^{\infty} (a_n T_{11}^n(\varepsilon) + b_n T_{12}^n(\varepsilon)) e^{in\theta}, \quad (85)$$

$$\delta t_\theta(x) = -\frac{2\mu}{\varepsilon^2} \sum_{n=-\infty}^{\infty} (a_n T_{41}^n(\varepsilon) + b_n T_{42}^n(\varepsilon)) e^{in\theta}, \quad (86)$$

where  $a_n$  and  $b_n$  are the constants determined by considering the boundary condition, and  $U_i(r)$ ,  $V_i(r)$ , and  $T_{ji}(r)$  ( $i \in \{1, 2\}$ ,  $j \in \{1, 2, 4\}$ ) are defined using the Hankel function of the first kind of order  $n$ ,  $H_n^{(1)}$ , as follows:

$$U_1^n(r) = -nH_n^{(1)}(k_L r) + k_L r H_{n-1}^{(1)}(k_L r), \quad (87)$$

$$U_2^n(r) = inH_n^{(1)}(k_T r), \quad (88)$$

$$V_1^n(r) = inH_n^{(1)}(k_L r), \quad (89)$$

$$V_2^n(r) = nH_n^{(1)}(k_T r) - k_T r H_{n-1}^{(1)}(k_T r), \quad (90)$$

$$T_{11}^n(r) = \left( n^2 + n - \frac{1}{2} k_T^2 r^2 \right) H_n^{(1)}(k_L r) - k_L r H_{n-1}^{(1)}(k_L r), \quad (91)$$

$$T_{12}^n(r) = -in \left( (n+1)H_n^{(1)}(k_T r) - k_T r H_{n-1}^{(1)}(k_T r) \right), \quad (92)$$

$$T_{21}^n(r) = - \left( n^2 + n + \frac{\lambda}{2\mu} k_L^2 r^2 \right) H_n^{(1)}(k_L r) + k_L r H_{n-1}^{(1)}(k_L r), \quad (93)$$

$$T_{22}^n(r) = in \left( (n+1)H_n^{(1)}(k_T r) - k_T r H_{n-1}^{(1)}(k_T r) \right), \quad (94)$$

$$T_{41}^n(r) = -in \left( (n+1)H_n^{(1)}(k_L r) - k_L r H_{n-1}^{(1)}(k_L r) \right), \quad (95)$$

$$T_{42}^n(r) = - \left( n^2 + n - \frac{1}{2} k_T^2 r^2 \right) H_n^{(1)}(k_T r) + k_T r H_{n-1}^{(1)}(k_T r), \quad (96)$$

where

$$k_T = \frac{\omega}{C_T}, \quad k_L = \frac{\omega}{C_L}. \quad (97)$$

From boundary condition (77),  $t_i$  can be expressed as,

$$t_i(x) = \sigma_{ij}^0 n_j(x) + O(\varepsilon). \quad (98)$$

Then, translate (98) into polar coordinate system, the  $r$ -direction component  $t_r$  and  $\theta$ -direction component  $t_\theta$  can be expressed as follows,

$$t_r(x) = -c_0 - c_2 e^{2i\theta} - c_{-2} e^{-2i\theta} + O(\varepsilon), \quad (99)$$

$$t_\theta(x) = -ic_2 e^{2i\theta} + ic_{-2} e^{-2i\theta} + O(\varepsilon), \quad (100)$$

where

$$n_1 = -\cos\theta, \quad (101)$$

$$n_2 = -\sin\theta. \quad (102)$$

and

$$c_0 = \frac{1}{2} (\sigma_{11}^0 + \sigma_{22}^0), \quad (103)$$

$$c_{\pm 2} = \frac{1}{4} (\sigma_{11}^0 - \sigma_{22}^0 \mp 2i \sigma_{12}^0) \quad (104)$$

Using the boundary condition Eq.(77), we compare the coefficients of  $e^{in\theta}$  in (85) and (98), and (86) and (100) for each

$n$ . Considering the orthogonality of  $\{e^{in\theta}\}_n$ ,  $a_n$  and  $b_n$  can be determined as follows.

$$a_0 = \frac{c_0 T_{42}^0(\varepsilon) \varepsilon^2}{2\mu (T_{12}^0(\varepsilon) T_{41}^0(\varepsilon) - T_{11}^0(\varepsilon) T_{42}^0(\varepsilon))} + O(\varepsilon^3) \quad (105)$$

$$a_{\pm 2} = \frac{c_{\pm 2} (T_{42}^{\pm 2}(\varepsilon) \mp iT_{12}^{\pm 2}(\varepsilon)) \varepsilon^2}{2\mu (T_{12}^{\pm 2}(\varepsilon) T_{41}^{\pm 2}(\varepsilon) - T_{11}^{\pm 2}(\varepsilon) T_{42}^{\pm 2}(\varepsilon))} + O(\varepsilon^3), \quad (106)$$

$$a_n = O(\varepsilon^3), \quad (n \notin \{-2, 0, 2\}), \quad (107)$$

$$b_0 = -\frac{c_0 T_{41}^0(\varepsilon) \varepsilon^2}{2\mu (T_{12}^0(\varepsilon) T_{41}^0(\varepsilon) - T_{11}^0(\varepsilon) T_{42}^0(\varepsilon))} + O(\varepsilon^3), \quad (108)$$

$$b_{\pm 2} = -\frac{c_{\pm 2} (T_{41}^{\pm 2}(\varepsilon) \mp iT_{11}^{\pm 2}(\varepsilon)) \varepsilon^2}{2\mu (T_{12}^{\pm 2}(\varepsilon) T_{41}^{\pm 2}(\varepsilon) - T_{11}^{\pm 2}(\varepsilon) T_{42}^{\pm 2}(\varepsilon))} + O(\varepsilon^3), \quad (109)$$

$$b_n = O(\varepsilon^3), \quad (n \notin \{-2, 0, 2\}) \quad (110)$$

Substituting equations from Eq.(105) to (110) into Eqs.(83) and (84), and evaluating the asymptotic expansions for  $\varepsilon \rightarrow 0$ , we obtain  $\delta u_r$  and  $\delta u_\theta$  on  $\Gamma_\varepsilon$  as follows:

$$\begin{aligned} \delta u_r|_{r=\varepsilon} &= \frac{1}{\varepsilon} \left[ (a_0 U_1^0(\varepsilon) + b_0 U_2^0(\varepsilon)) \right. \\ &\quad + (a_2 U_1^2(\varepsilon) + b_2 U_2^2(\varepsilon)) e^{2i\theta} \\ &\quad \left. + (a_{-2} U_1^{-2}(\varepsilon) + b_{-2} U_2^{-2}(\varepsilon)) e^{-2i\theta} \right] + O(\varepsilon^2) \\ &= \frac{1}{2\mu} \left[ c_0 + \frac{k_T^2 + k_L^2}{k_T^2 - k_L^2} (c_2 e^{2i\theta} + c_{-2} e^{-2i\theta}) \right] \varepsilon + O(\varepsilon^2) \\ &= \frac{\varepsilon}{4\mu (k_T^2 - k_L^2)} \left\{ (k_T^2 - k_L^2) (\sigma_{11}^0 + \sigma_{22}^0) \right. \\ &\quad \left. + (k_T^2 + k_L^2) [(\sigma_{11}^0 - \sigma_{22}^0) \cos 2\theta + 2\sigma_{12}^0 \sin 2\theta] \right\} \\ &\quad + O(\varepsilon^2), \quad (111) \end{aligned}$$

$$\begin{aligned} \delta u_\theta|_{r=\varepsilon} &= \frac{1}{\varepsilon} \left\{ [a_0 V_1^0(\varepsilon) + b_0 V_2^0(\varepsilon)] \right. \\ &\quad + [a_2 V_1^2(\varepsilon) + b_2 V_2^2(\varepsilon)] e^{2i\theta} \\ &\quad \left. + [a_{-2} V_1^{-2}(\varepsilon) + b_{-2} V_2^{-2}(\varepsilon)] e^{-2i\theta} \right\} + O(\varepsilon^2) \\ &= \frac{i}{2\mu} \frac{k_T^2 + k_L^2}{k_T^2 - k_L^2} (c_2 e^{2i\theta} + c_{-2} e^{-2i\theta}) \varepsilon + O(\varepsilon^2) \\ &= \frac{(k_T^2 + k_L^2) [ -(\sigma_{11}^0 - \sigma_{22}^0) \sin 2\theta + 2\sigma_{12}^0 \cos 2\theta ]}{4\mu (k_T^2 - k_L^2)} \varepsilon \\ &\quad + O(\varepsilon^2). \quad (112) \end{aligned}$$

By transforming Eqs.(111) and (112) back into  $(x_1, x_2)$  coordinates, we obtain

$$\begin{aligned} \delta u_1|_{r=\varepsilon} &= \delta u_r|_{r=\varepsilon} \cos \theta - \delta u_\theta|_{r=\varepsilon} \sin \theta \\ &= \frac{(k_T^2 \sigma_{11}^0 - k_L^2 \sigma_{22}^0) \varepsilon \cos \theta + (k_T^2 + k_L^2) \sigma_{12}^0 \varepsilon \sin \theta}{2\mu (k_T^2 - k_L^2)} \\ &\quad + O(\varepsilon^2) \\ &= \frac{(k_T^2 \sigma_{11}^0 - k_L^2 \sigma_{22}^0) x_1 + (k_T^2 + k_L^2) \sigma_{12}^0 x_2}{2\mu (k_T^2 - k_L^2)} + O(\varepsilon^2) \\ &= \frac{1}{2\mu (\lambda + \mu)} \left\{ [(\lambda + 2\mu) \sigma_{11}^0 - \mu \sigma_{22}^0] x_1 \right. \\ &\quad \left. + (\lambda + 3\mu) \sigma_{12}^0 x_2 \right\} + O(\varepsilon^2), \quad (113) \end{aligned}$$

$$\begin{aligned} \delta u_2|_{r=\varepsilon} &= \delta u_r|_{r=\varepsilon} \sin \theta + \delta u_\theta|_{r=\varepsilon} \cos \theta \\ &= \frac{(k_T^2 + k_L^2) \sigma_{12}^0 \varepsilon \cos \theta + (k_T^2 \sigma_{22}^0 - k_L^2 \sigma_{11}^0) \varepsilon \sin \theta}{2\mu (k_T^2 - k_L^2)} \\ &\quad + O(\varepsilon^2) \\ &= \frac{(k_T^2 + k_L^2) \sigma_{12}^0 x_1 + (k_T^2 \sigma_{22}^0 - k_L^2 \sigma_{11}^0) x_2}{2\mu (k_T^2 - k_L^2)} + O(\varepsilon^2) \\ &= \frac{1}{2\mu (\lambda + \mu)} \left\{ (\lambda + 3\mu) \sigma_{21}^0 x_1 \right. \\ &\quad \left. + [(\lambda + 2\mu) \sigma_{22}^0 - \mu \sigma_{11}^0] x_2 \right\} + O(\varepsilon^2) \quad (114) \end{aligned}$$

Thus,  $\delta u_i$  on  $\Gamma_\varepsilon$  can be written using index notation as follows:

$$\delta u_i|_{r=\varepsilon} = \frac{1}{2\mu (\lambda + \mu)} [(\lambda + 3\mu) \sigma_{ij}^0 x_j - \mu \sigma_{jj}^0 x_i] + O(\varepsilon^2) \quad (115)$$

By using Eq.(115), the second term of the right-hand side of Eq.(39) can be obtained as follows:

$$\begin{aligned} \int_{\Gamma_\varepsilon} \tilde{t}_i \delta u_i d\Gamma &= \frac{1}{2\mu (\lambda + \mu)} \int_{\Gamma_\varepsilon} [(\lambda + 3\mu) \sigma_{ij}^0 x_i - \mu \sigma_{jj}^0 x_i] \tilde{t}_i d\Gamma \\ &\quad + O(\varepsilon^3) \\ &= -\frac{\varepsilon}{2\mu (\lambda + \mu)} \int_{\Gamma_\varepsilon} [(\lambda + 3\mu) \sigma_{ij}^0 n_j - \mu \sigma_{jj}^0 n_i] \tilde{\sigma}_{ik}^0 n_k d\Gamma \\ &\quad + O(\varepsilon^3) \\ &= -\frac{\varepsilon}{2\mu (\lambda + \mu)} \tilde{\sigma}_{ik}^0 [(\lambda + 3\mu) \sigma_{ij}^0 \int_{\Gamma_\varepsilon} n_j n_k d\Gamma \\ &\quad - \mu \sigma_{jj}^0 \int_{\Gamma_\varepsilon} n_i n_k d\Gamma] + O(\varepsilon^3) \\ &= -\frac{\pi \varepsilon^2}{2\mu (\lambda + \mu)} \tilde{\sigma}_{ik}^0 [(\lambda + 3\mu) \sigma_{ij}^0 \delta_{jk} - \mu \sigma_{jj}^0 \delta_{ik}] + O(\varepsilon^3) \\ &= -\frac{\pi \varepsilon^2}{2\mu (\lambda + \mu)} [(\lambda + 3\mu) \sigma_{ij}^0 \tilde{\sigma}_{ij}^0 - \mu \tilde{\sigma}_{ii}^0 \sigma_{jj}^0] + O(\varepsilon^3), \quad (116) \end{aligned}$$

where

$$\int_{\Gamma_\varepsilon} n_i n_j d\Gamma = \pi \varepsilon \delta_{ij} \quad (117)$$

is used.

By substituting Eqs.(116) and (75) into (39),  $\delta J$  is obtained in its explicit form as

$$\begin{aligned} \delta J &= \pi \varepsilon^2 \text{Re} \left[ \frac{\lambda + 2\mu}{4\mu (\lambda + \mu)} (4\sigma_{ij}^0 \tilde{\sigma}_{ij}^0 - \sigma_{ii}^0 \tilde{\sigma}_{jj}^0) - \rho \omega^2 u_i^0 \tilde{u}_i^0 \right] \\ &\quad + O(\varepsilon^3). \quad (118) \end{aligned}$$

Therefore, the topological derivative is obtained as

$$\begin{aligned} \mathcal{T}(x^0) &= \lim_{\varepsilon \rightarrow 0} \frac{\delta J}{\pi \varepsilon^2} \\ &= \text{Re} \left[ \frac{\lambda + 2\mu}{4\mu (\lambda + \mu)} (4\sigma_{ij}^0 \tilde{\sigma}_{ij}^0 - \sigma_{ii}^0 \tilde{\sigma}_{jj}^0) - \rho \omega^2 u_i^0 \tilde{u}_i^0 \right] \quad (119) \end{aligned}$$